

Revisiting $U_A(1)$ restoration from meson masses and mixing angles in the 2+1 flavor modified Polyakov quark meson model

Suraj Kumar Rai and Vivek Kumar Tiwari*

Department of Physics, University of Allahabad, Allahabad 211002, India.

(Dated: December 18, 2018)

We are investigating $U_A(1)$ symmetry restoration by introducing a temperature dependent coefficient $c(T)$ for the Kobayashi-Maskawa-'t Hooft determinant (KMT) term in the 2+1 flavor Polyakov loop quark meson model with fermionic vacuum correction term (PQMVT). The PQMVT model setting is effectively Quantum Chromodynamics (QCD)-like due to proper accounting of the renormalized contribution of the divergent fermionic vacuum fluctuation at one loop level. The lattice QCD (LQCD) simulations for the pion and a_0 - meson screening masses, suggest strong suppression of the coefficient $c(T)$ near the pseudocritical temperature of the chiral crossover. Comparing the results for the temperature dependent coupling strength $c(T)$ with those of constant coupling c in the PQMVT model, we report significantly modified $U_A(1)$ symmetry restoration pattern in the PQMVT model. The interplay of chiral symmetry restoration and the $U_A(1)$ restoration trend also gets significantly modified. The role of the $U_A(1)$ anomaly in determining the isoscalar masses and mixing angles for the pseudoscalar (η and η') and scalar (σ and f_0) meson complex also gets significantly modified due to the temperature dependence of the coupling strength $c(T)$.

PACS numbers: 12.38.Aw, 11.30.Rd, 12.39.Fe, 11.10.Wx

I. INTRODUCTION

The normal hadronic matter under the extreme conditions of high temperature and/or density, turns into a collective form of matter known as the Quark Gluon Plasma (QGP) when the individual hadrons dissolve into their quark and gluon constituents [1–6]. Relativistic heavy ion collision experiments at RHIC (BNL), LHC (CERN) and the future CBM experiments at the FAIR facility (GSI-Darmstadt) aim to create and study such a collective state of matter. Study of the different aspects of this phase transition, is a tough and challenging task because Quantum Chromodynamics (QCD), the theory of strong interaction, becomes nonperturbative in the low energy limit.

It is well known that the basic quantum chromodynamics (QCD) Lagrangian has the global $SU_{R+L}(3) \times SU_{R-L}(3) \times U_V(1) \times U_A(1)$ symmetry. Here Axial vector $A = R - L$ and Vector $V = R + L$. The $U_V(1)$ symmetry gives baryon number conservation. The QCD vacuum reveals itself through the process of spontaneous breakdown of chiral symmetry $SU_A(3)$ for the massless quarks in the low energy limit of QCD. Chiral condensate works as an order parameter and one gets eight massless pseudoscalar mesons as Goldstone bosons for the low energy hadronic vacuum of the QCD. For small quark masses in the real QCD, the mesons become pseudo-Goldstone bosons with small non zero masses in comparison to other hadrons. Melting of

chiral condensate at higher temperature T_c leads to chiral symmetry restoring phase transition for zero quark mass chiral limit. For 2+1 flavor of light quark masses, the phase transition turns into a rapid crossover. Lattice QCD simulations show that the pseudo-critical temperature for such chiral crossover is $T_c = 154 \pm 9$ [7–9].

QCD also has $U_A(1)$ axial symmetry at the classical level which is broken explicitly by the quantum anomaly as shown by 't Hooft [10]. In QCD vacuum, Instanton effects explicitly break the $U_A(1)$ to $Z_A(3)$. $U_A(1)$ symmetry breaking can be understood in terms of Kobayashi-Maskawa-'t Hooft (KMT) determinant [10, 11] describing the flavor mixing six quark interaction that gets contributions from fluctuations in the topological charge. Flavor mixing removes the degeneracy among several mesons. The pseudoscalar singlet η' meson acquires a mass of about 1 GeV. In the absence of $U_A(1)$ anomaly, η' would have been degenerate with π in $U(3)$ as a ninth Goldstone boson in the spontaneously broken chirally symmetric phase.

Since the fluctuations in the topological charge are suppressed at temperatures far above the chiral crossover temperature T_c [12, 13], it is expected that the axial anomaly vanishes and $U_A(1)$ symmetry gets effectively restored for temperature $T_{U(1)} \gg T_c$. Shuryak [14] has discussed two scenarios: the complete chiral symmetry $SU_A(3) \times U_A(1)$ is restored in scenario one for $T_{U(1)} \gg T_c$ well inside the quark gluon plasma region and in scenario two $T_{U(1)} \sim T_c$. Further, it has been argued that mass splitting between pion and pseudoscalar singlet meson could become small immediately above the chiral crossover [15]. In Ref [16, 17], it is reported that the in-medium mass of pseudoscalar singlet meson drops by

*Electronic address: surajrai050@gmail.com; Electronic address: vivekkr@gmail.com

at least 200 MeV which supposedly is an experimental signature of effective restoration of $U_A(1)$ symmetry .

Some lattice QCD calculations have addressed the issue of effective restoration of $U_A(1)$ symmetry. Recently $U_A(1)$ restoration was explored by computing the degeneration of pion and a_0 -meson screening masses using improved p^4 staggered fermions [18]. In a two-flavor simulation with overlap and domain wall fermions [19, 20], the correlators of pion and pseudo-scalar singlet meson have been observed to be degenerate in the chiral symmetric phase . For 2+1 domain wall fermions Ref [21, 22] find effective restoration of $U_A(1)$ at a larger temperature of 196 MeV while Refs [23, 24] do not see restoration even at 1.5 times the crossover temperature using highly improved staggered fermions. The interplay of $U_A(1)$ axial symmetry restoration and chiral crossover transition has been explored in several effective model settings like Dyson-Schwinger approach using quark-gluon interaction [25–28], in the Nambu-Jona-Lasinio (NJL) model [29–34] and linear sigma models [35–38] which become quark-meson (QM) models [39–42] when coupled with quarks , in the Polyakov loop augmented Nambu-Jona-Lasinio (PNJL) models and Polyakov loop enhanced quark-meson (PQM) models. PNJL and PQM models combine the features of spontaneous breakdown of both chiral symmetry as well as the center $Z(3)$ symmetry of QCD in one single model (see for example [43–74]). In these models chiral condensate and Polyakov loop are simultaneously coupled to the quark degrees of freedom. In the high temperature/density regime, QCD vacuum shows color confinement-deconfinement phase transition for the infinitely heavy quarks where the centre symmetry $Z(3)$ of color gauge group $SU_c(3)$ gets spontaneously broken and the expectation value of the Wilson line (Polyakov loop) serves as the order parameter [75] as it is related to the free energy of a static color charge . Since the center symmetry is always explicitly broken in the presence of dynamical quarks in the system, one regards the Polyakov loop as an approximate order parameter for the confinement-deconfinement transition [76, 77].

It is still an interesting and open question of QCD whether the phenomenon of $U_A(1)$ restoration is in some way linked to the $SU_A(3)$ chiral symmetry restoration [78, 79]. One of the present author in the 2+1 flavor PQM model [45–48] explored the effect of confinement physics i.e that of the Polyakov loop potential on the temperature dependence of the scalar and pseudo scalar meson mass spectrum and the mixing angles above chiral crossover temperature T_c in the presence as well as absence of $U_A(1)$ axial anomaly. Earlier in the 2+1 flavor QM model, Schaefer et. al. [39, 40] had studied the interplay of $SU(3)$ chiral symmetry and $U_A(1)$ axial symmetry at higher temperatures. Skokov et. al. further enriched and improved the two flavor QM model by including renormalized fermionic vacuum fluctuation [80] in its thermodynamic potential. It becomes an effective QCD-like model because now it can reproduce

the second order chiral phase transition at $\mu = 0$ as expected from the universality arguments [81] for the two massless flavors of QCD. Earlier works [82–85] have also investigated the fermionic vacuum correction and its effect. Here, it is relevant to point out that the $U_A(1)$ symmetry and its relation to the chiral symmetry in the QM and PQM model has also been investigated in the powerful framework of nonperturbative functional renormalization group (FRG) method [86, 87] where the bosonic and fermionic quantum fluctuations are included in the FRG effective action through running the RG scale from the ultraviolet scale to the infrared limit, which, as an advantage, can automatically guarantee the Nambu-Goldstone theorem in the symmetry breaking phase .

In recent series of work [88, 89], one of the present author generalized the inclusion of renormalized fermionic vacuum correction in the two flavor QM and PQM models to the non-zero chemical potentials and compared the size of critical region around the shifted critical end point in the phase diagram. In earlier works, the renormalization scale independence of the model parameters and meson masses used to be implemented numerically [90, 91] when the renormalized contribution of the divergent fermionic vacuum fluctuation at one loop level was incorporated in the model. Very recently, one of the present author has refined the 2+1 flavor QM and PQM models further by finding explicit renormalization scale independent analytical expressions for the model parameters, meson masses and mixing angles and then investigated the effect of fermionic vacuum correction, on the interplay of $SU_A(3)$ chiral symmetry and $U_A(1)$ symmetry restoration when the masses of chiral partners become degenerate as the parity doubling takes place on increasing the temperature through T_c [92].

In this paper, we are investigating the $U_A(1)$ symmetry restoration and its interplay with the chiral symmetry restoration by introducing a temperature dependent coefficient $c(T)$ for the Kobayashi-Maskawa-'t Hooft (KMT) determinant term in the 2+1 flavor Polyakov loop quark meson model with fermionic vacuum correction term (PQMVT). The lattice QCD (LQCD) simulations for the pion and a_0 - meson screening masses, suggest strong suppression of the coefficient $c(T)$ near the pseudocritical temperature of the chiral crossover [18]. The effect of temperature dependence of the KMT coupling strength on the $U_A(1)$ symmetry restoration has already been studied in the 2+1 flavor entanglement-PNJL (EPNJL) model [93, 94]. It is instructive to have such a detailed investigation in PQMVT model also since mesons in the NJL model are generated by some prescription [30] and the η' is not a well defined quantity [79] which becomes unbound for higher temperatures .

This paper has the following arrangement . Sec.II, explains the formulation of the model. Sec. III describes the mean field grand potential. The subsection III A gives the details of scale independent effective potential after

renormalizing the one loop fermionic vacuum fluctuation. The model parameters are also given. The Sec.IV gives the model formulae of meson masses and mixing angles in a finite temperature/density medium. In Sec.V, we will be discussing the numerical results and plots for temperature variations of meson masses and mixing angles. Summary and conclusion is presented in the last Sec.VI.

II. MODEL FORMULATION

In the model [45–48], three flavor of quarks are coupled to the $SU_V(3) \times SU_A(3)$ symmetric mesonic fields together with spatially constant temporal gauge field represented by the Polyakov loop potential. Thermal expectation value of color trace of Wilson loop in temporal direction defines the Polyakov loop field Φ as

$$\Phi = \frac{1}{N_c} \langle \text{Tr}_c L(\vec{x}) \rangle, \quad \bar{\Phi} = \frac{1}{N_c} \langle \text{Tr}_c L^\dagger(\vec{x}) \rangle \quad (1)$$

where $L(\vec{x})$ is a matrix in the fundamental representation of the $SU_c(3)$ color gauge group.

$$L(\vec{x}) = \mathcal{P} \exp \left[i \int_0^\beta d\tau A_0(\vec{x}, \tau) \right] \quad (2)$$

Here \mathcal{P} is path ordering, A_0 is the temporal vector field and $\beta = T^{-1}$ [75].

The model Lagrangian is written in terms of quarks, mesons, couplings and Polyakov loop potential $\mathcal{U}(\Phi, \bar{\Phi}, T)$.

$$\mathcal{L}_{PQM} = \mathcal{L}_{QM} - \mathcal{U}(\Phi, \bar{\Phi}, T) \quad (3)$$

where the Lagrangian in Quark Meson Chiral Sigma model

$$\mathcal{L}_{QM} = \bar{q}_f (i\gamma^\mu D_\mu - g T_a (\sigma_a + i\gamma_5 \pi_a)) q_f + \mathcal{L}_m \quad (4)$$

Quarks couple with the uniform temporal background gauge field as the following $D_\mu = \partial_\mu - iA_\mu$ and $A_\mu = \delta_{\mu 0} A_0$ (Polyakov gauge), where $A_\mu = g_s A_\mu^a \lambda^a / 2$ with vector potential A_μ^a for color gauge field. g_s is the $SU_c(3)$ gauge coupling. λ_a are Gell-Mann matrices in the color space, a runs from $1 \cdots 8$. $q_f = (u, d, s)^T$ denotes the quarks of three flavors and three colors. T_a represent 9 generators of $U(3)$ flavor symmetry with $T_a = \frac{\lambda_a}{2}$ and $a = 0, 1 \cdots 8$, here λ_a are standard Gell-Mann matrices in flavor space with $\lambda_0 = \sqrt{\frac{2}{3}} \mathbf{1}$. g is the flavor blind Yukawa coupling that couples the three flavor of quarks with nine mesons in the scalar ($\sigma_a, J^P = 0^+$) and pseudo scalar ($\pi_a, J^P = 0^-$) sectors. The quarks acquire mass though spontaneous breakdown of chiral symmetry.

The mesonic part of the Lagrangian has the following form

$$\begin{aligned} \mathcal{L}_m = & \text{Tr} (\partial_\mu M^\dagger \partial^\mu M) - m^2 \text{Tr} (M^\dagger M) - \lambda_1 [\text{Tr} (M^\dagger M)]^2 \\ & - \lambda_2 \text{Tr} (M^\dagger M)^2 + c [\det(M) + \det(M^\dagger)] \\ & + \text{Tr} [H(M + M^\dagger)]. \end{aligned} \quad (5)$$

The chiral field M is a 3×3 complex matrix comprising of the nine scalars σ_a and the nine pseudo scalar π_a mesons.

$$M = T_a \xi_a = T_a (\sigma_a + i\pi_a) \quad (6)$$

The generators follow $U(3)$ algebra $[T_a, T_b] = if_{abc} T_c$ and $\{T_a, T_b\} = d_{abc} T_c$ where f_{abc} and d_{abc} are standard antisymmetric and symmetric structure constants respectively with $f_{ab0} = 0$ and $d_{ab0} = \sqrt{\frac{2}{3}} \mathbf{1} \delta_{ab}$ and matrices are normalized as $\text{Tr}(T_a T_b) = \frac{\delta_{ab}}{2}$.

The $SU_L(3) \times SU_R(3)$ chiral symmetry is explicitly broken by the explicit symmetry breaking term

$$H = T_a h_a \quad (7)$$

Here H is a 3×3 matrix with nine external parameters. The ξ field which denotes both the scalar as well as pseudo scalar mesons, picks up the nonzero vacuum expectation value, $\bar{\xi}$ for the scalar mesons due to the spontaneous breakdown of the chiral symmetry while the pseudo scalar mesons have zero vacuum expectation value. Since $\bar{\xi}$ must have the quantum numbers of the vacuum, explicit breakdown of the chiral symmetry is only possible with three nonzero parameters h_0 , h_3 and h_8 . We are neglecting isospin symmetry breaking hence we choose $h_0, h_8 \neq 0$. This leads to the $2 + 1$ flavor symmetry breaking scenario with nonzero condensates $\bar{\sigma}_0$ and $\bar{\sigma}_8$. Apart from h_0 and h_8 , the other parameters in the model are five in number. These are the squared tree-level mass of the meson fields m^2 , quartic coupling constants λ_1 and λ_2 , a Yukawa coupling g and a cubic coupling c which is constant in the QM/PQM model and accounts for the $U_A(1)$ axial anomaly of the QCD vacuum.

The density of the instantons gets screened by the medium at finite temperature T . Since the coupling c of the KMT interaction is proportional to the instanton density, it gets reduced as T increases. In this paper, we consider the introduction of the following temperature dependent coefficient $c(T)$ for the Kobayashi-Maskawa-'t Hooft (KMT) determinant term in the PQM model with vacuum term.

$$c(T) = \begin{cases} c(0), & (T < T_1) \\ c(0) \exp[-\frac{(T - T_1)^2}{b_1^2}], & (T > T_1) \end{cases} \quad (8)$$

The above parameterization of KMT coupling strength was introduced very recently for exploring the $U_A(1)$ symmetry restoration in the context of the

entanglement-PNJL (EPNJL) model [93, 94] where the parameters T_1 and b_1 are determined from LQCD data on pion and a_0 -meson screening masses. The T dependence of Eq. (8) is consistent with the Pisarski and Yaffe suppression of the instanton density for high $T \geq 2T_c$ and is similar to the Woods-Saxon form [14, 95].

A. Polyakov Loop Potential

The effective Polyakov loop potential $\mathcal{U}(\Phi, \bar{\Phi}, T)$ is constructed such that it reproduces thermodynamics of pure glue theory on the lattice for temperatures upto about twice the deconfinement phase transition temperature. The simplest polynomial form of Polyakov loop effective potential based on Landau-Ginzburg ansatz is written as [54]

$$\frac{\mathcal{U}_{\text{Poly}}(\Phi, \bar{\Phi}, T)}{T^4} = -\frac{b_2(T)}{2}\bar{\Phi}\Phi - \frac{b_3}{6}(\bar{\Phi} + \Phi^3) + \frac{b_4}{4}(\bar{\Phi}\Phi)^2 \quad (9)$$

Later, the Jacobian of transformation from the matrix valued field L to the complex valued field Φ known as the VanderMonde (VM) term was included and an improved ansatz was proposed [55, 56]. In this work, the form of Polyakov loop potential has been chosen as in Ref. [56]

$$\frac{\mathcal{U}_{\text{Poly-VM}}(\Phi, \bar{\Phi}, T)}{T^4} = \frac{\mathcal{U}_{\text{Poly}}(\Phi, \bar{\Phi}, T)}{T^4} - \kappa \ln[1 - 6\bar{\Phi}\Phi + 4(\bar{\Phi}^3 + \Phi^3) - 3(\bar{\Phi}\Phi)^2] \quad (10)$$

where the parameters are the following

$$b_2(T) = a_0 + a_1 \left(\frac{T_0}{T}\right) + a_2 \left(\frac{T_0}{T}\right)^2 + a_3 \left(\frac{T_0}{T}\right)^3.$$

The parameters in $b_2(T)$ and coefficients b_3, b_4 are found by fitting the pure gauge lattice data as in [54]

$$\begin{aligned} a_0 &= 6.75, & a_1 &= -1.95, & b_3 &= 0.75 \\ a_2 &= 2.625, & a_3 &= -7.44, & b_4 &= 7.5 \end{aligned}$$

The parameter $\kappa = 0.1$ has been fixed by fitting the Wuppertal group lattice data [7] for scaled chiral order parameter temperature variation to the corresponding temperature variation in our PQMVT model calculation. For pure gauge Yang Mills theory, the critical temperature of deconfinement phase transition is $T_0 = 270$ MeV. In the presence of dynamical quarks T_0 is directly linked to the mass-scale Λ , the parameter which has a flavor and chemical potential dependence in full dynamical QCD and $T_0 \rightarrow T_0(N_f, \mu)$. The N_f and μ dependence of T_0 [43, 44, 49, 50, 90] is written as

$$T_0(N_f, \mu) = T_\tau e^{-1/(\alpha_0 b(N_f, \mu))} \quad (11)$$

where $T_\tau = 1.77$ GeV denotes the τ scale and $\alpha_0 = \alpha(\Lambda)$ the gauge coupling at some UV scale Λ . The μ -dependent running coupling reads

$$b(N_f, \mu) = b(N_f) - b_\mu \frac{\mu^2}{T_\tau^2}, \quad (12)$$

the factor $b_\mu \simeq \frac{16}{\pi} N_f$. Refs. [43, 49] contain the details of formula. Our present computations have been done at $\mu = 0$ and $T_0 = 187$ for 2+1 quark flavors [43].

III. GRAND POTENTIAL IN THE MEAN FIELD APPROACH

We are considering a spatially uniform system in thermal equilibrium at finite temperature T and quark chemical potential μ_f ($f = u, d$ and s). The partition function is written as the path integral over quark/antiquark and meson fields [39, 45]

$$\begin{aligned} \mathcal{Z} &= \text{Tr} \exp[-\beta(\hat{\mathcal{H}} - \sum_{f=u,d,s} \mu_f \hat{\mathcal{N}}_f)] \\ &= \int \prod_a \mathcal{D}\sigma_a \mathcal{D}\pi_a \int \mathcal{D}q \mathcal{D}\bar{q} \exp \left[- \int_0^\beta d\tau \int_V d^3x \right. \\ &\quad \left. \left(\mathcal{L}_{\mathcal{QM}}^\mathcal{E} + \sum_{f=u,d,s} \mu_f \bar{q}_f \gamma^0 q_f \right) \right]. \end{aligned} \quad (13)$$

where V is the three dimensional volume of the system, $\beta = \frac{1}{T}$ and the superscript \mathcal{E} denotes the euclidean Lagrangian. For three quark flavors, in general, the three quark chemical potentials are different. In this work, we assume that $SU_V(2)$ symmetry is preserved and neglect the small difference in masses of u and d quarks. Thus the quark chemical potential for the u and d quarks become equal $\mu_x = \mu_u = \mu_d$. The strange quark chemical potential is $\mu_y = \mu_s$. Further we consider symmetric quark matter and net baryon number to be zero.

Here, the partition function is evaluated in the mean-field approximation [39, 40, 45]. We replace meson fields by their expectation values $\langle M \rangle = T_0 \bar{\sigma}_0 + T_8 \bar{\sigma}_8$ and neglect both thermal as well as quantum fluctuations of meson fields while quarks and anti quarks are retained as quantum fields. Now following the standard procedure as given in Refs. [43, 54, 66, 96], one can obtain the expression of grand potential as the sum of pure gauge field contribution $\mathcal{U}(\Phi, \bar{\Phi}, T)$, meson contribution and quark/antiquark contribution evaluated in the presence of Polyakov loop,

$$\begin{aligned} \Omega_{\text{MF}}(T, \mu) &= -\frac{T \ln Z}{V} = U(\sigma_x, \sigma_y) + \mathcal{U}_{\text{Poly-VM}}(\Phi, \bar{\Phi}, T) \\ &\quad + \Omega_{\bar{q}q}(T, \mu) \end{aligned} \quad (14)$$

The mesonic potential $U(\sigma_x, \sigma_y)$ is obtained from the $U(\sigma_0, \sigma_8)$ after transforming the original singlet-octet (0, 8) basis of condensates to the non strange-strange basis

(x, y) as in Refs. [36, 39, 45, 90]. We write the mesonic potential as

$$U(\sigma_x, \sigma_y) = \frac{m^2}{2} (\sigma_x^2 + \sigma_y^2) - h_x \sigma_x - h_y \sigma_y - \frac{c}{2\sqrt{2}} \sigma_x^2 \sigma_y + \frac{\lambda_1}{2} \sigma_x^2 \sigma_y^2 + \frac{1}{8} (2\lambda_1 + \lambda_2) \sigma_x^4 + \frac{1}{8} (2\lambda_1 + 2\lambda_2) \sigma_y^4 \quad (15)$$

where

$$\sigma_x = \sqrt{\frac{2}{3}} \bar{\sigma}_0 + \frac{1}{\sqrt{3}} \bar{\sigma}_8, \quad (16)$$

$$\sigma_y = \frac{1}{\sqrt{3}} \bar{\sigma}_0 - \sqrt{\frac{2}{3}} \bar{\sigma}_8. \quad (17)$$

The chiral symmetry breaking external fields (h_x, h_y) are written in terms of (h_0, h_8) analogously.

Further the non strange and strange quark/antiquark decouple and the quark masses are

$$m_x = g \frac{\sigma_x}{2}, \quad m_y = g \frac{\sigma_y}{\sqrt{2}} \quad (18)$$

Quarks become massive in symmetry broken phase because of non zero vacuum expectation values of the condensates. The quark/antiquark contribution, in the presence of Polyakov loop potential, is written as

$$\Omega_{\bar{q}q}(T, \mu) = \Omega_{\bar{q}q}^{\text{vac}} + \Omega_{\bar{q}q}^{\text{T}} = -2 \sum_{f=u,d,s} \int \frac{d^3 p}{(2\pi)^3} \left[N_c E_f \theta(\Lambda^2 - \vec{p}^2) + T \{ \ln g_f^+ + \ln g_f^- \} \right] \quad (19)$$

The first term of the Eq. (19) represents the fermion vacuum one loop contribution, regularized by the ultraviolet cutoff Λ . The expressions g_f^+ and g_f^- are defined in the second term after taking trace over the color space

$$g_f^+ = \left[1 + 3\Phi e^{-E_f^+/T} + 3\bar{\Phi} e^{-2E_f^+/T} + e^{-3E_f^+/T} \right] \quad (20)$$

$$g_f^- = \left[1 + 3\bar{\Phi} e^{-E_f^-/T} + 3\Phi e^{-2E_f^-/T} + e^{-3E_f^-/T} \right] \quad (21)$$

$E_f^\pm = E_f \mp \mu$ and E_f is the flavor dependent single particle energy of quark/antiquark and m_f is the mass of the given quark flavor.

$$E_f = \sqrt{p^2 + m_f^2} \quad (22)$$

A. Effective Potential with Renormalized Fermionic Vacuum Term

The first term of Eq. (19) can be properly renormalized using the dimensional regularization scheme as done for two flavor case in Ref.[80, 88, 89] and three flavor case in Ref.[90–92]. The essential steps are given in Ref.[92].

The renormalized fermion vacuum loop contribution at one-loop order [92, 97] is written as :

$$\Omega_{\bar{q}q}^{\text{vac}} = - \sum_{f=u,d,s} \frac{N_c}{8\pi^2} m_f^4 \ln \left(\frac{m_f}{M} \right) \quad (23)$$

We note that the Polyakov loop potential and the temperature dependent part of the quark-antiquark contribution to the grand potential in Eq.(14) vanishes at $T = 0$ and $\mu = 0$. The Polyakov loop order parameter $\Phi = \bar{\Phi}$ becomes zero in the low temperature phase due to the phenomenon of color confinement and this makes the Polyakov loop potential $\mathcal{U}_{\text{Poly-VM}}(\Phi, \bar{\Phi}, T)$ zero at $T = 0$ in Eq.(10). When the fermionic vacuum loop contribution in the first term of Eq.(19), gets replaced by the appropriately renormalized term of Eq.(23), the grand potential in vacuum becomes the renormalization scale M dependent and we write [92] :

$$\Omega^M(\sigma_x, \sigma_y) = U(\sigma_x, \sigma_y) + \Omega_{\bar{q}q}^{\text{vac}} \quad (24)$$

The six unknown parameters m^2 , λ_1, λ_2 , h_x, h_y and c in the mesonic potential $U(\sigma_x, \sigma_y)$, are determined from the σ_x and σ_y dependent expressions of meson masses which are obtained by the double derivatives of the effective potential Eq.(24) with respect to different meson fields. The mathematical details for determining different parameters are given in the appendix A of Ref. [92] where the logarithmic M dependence of the term $\Omega_{\bar{q}q}^{\text{vac}}$ gives rise to a renormalization scale M dependent part λ_{2M} in the expression of the parameter $\lambda_2 = \lambda_{2s} + n + \lambda_{2+} + \lambda_{2M}$. λ_{2s} is the same old λ_2 parameter of the QM/PQM model in Ref. [36, 39, 45]. Here, $n = \frac{N_c g^4}{32\pi^2}$, $\lambda_{2+} = \frac{n f_\pi^2}{f_K(f_K - f_\pi)} \log \left\{ \frac{2f_K - f_\pi}{f_\pi} \right\}$ and $\lambda_{2M} = 4n \log \left\{ \frac{g(2f_K - f_\pi)}{2M} \right\}$. After substituting this value of λ_2 in the expression of $U(\sigma_x, \sigma_y)$ and writing all the terms of summation in $\Omega_{\bar{q}q}^{\text{vac}}$ expression explicitly, the Eq. (24) can be rewritten as:

$$\begin{aligned} \Omega^M(\sigma_x, \sigma_y) = & \frac{m^2}{2} (\sigma_x^2 + \sigma_y^2) - h_x \sigma_x - h_y \sigma_y - \frac{c}{2\sqrt{2}} \sigma_x^2 \sigma_y \\ & + \frac{\lambda_1}{4} (\sigma_x^4 + \sigma_y^4 + 2\sigma_x^2 \sigma_y^2) + \frac{(\lambda_{2v} + n + \lambda_{2M})}{8} (\sigma_x^4 + 2\sigma_y^4) \\ & - \frac{n\sigma_x^4}{2} \log \left(\frac{g\sigma_x}{2M} \right) - n\sigma_y^4 \log \left(\frac{g\sigma_y}{\sqrt{2}M} \right) \end{aligned} \quad (25)$$

here, $\lambda_{2v} = \lambda_{2s} + \lambda_{2+}$. After rearrangement of terms, we find that the logarithmic M dependence of λ_2 contained in λ_{2M} , completely cancels the scale dependence of all the terms in $\Omega_{\bar{q}q}^{\text{vac}}$. The chiral part of the total effective potential now becomes free of any renormalization scale dependence. It is reexpressed as [92]

$$\begin{aligned} \Omega(\sigma_x, \sigma_y) = & \frac{m^2}{2} (\sigma_x^2 + \sigma_y^2) - h_x \sigma_x - h_y \sigma_y - \frac{c}{2\sqrt{2}} \sigma_x^2 \sigma_y \\ & + \frac{\lambda_1}{2} \sigma_x^2 \sigma_y^2 + \frac{\lambda_1}{4} (\sigma_x^4 + \sigma_y^4) + \frac{(\lambda_{2v} + n)}{8} (\sigma_x^4 + 2\sigma_y^4) \\ & - \frac{n\sigma_x^4}{2} \log \left(\frac{\sigma_x}{(2f_K - f_\pi)} \right) - n\sigma_y^4 \log \left(\frac{\sqrt{2} \sigma_y}{(2f_K - f_\pi)} \right) \end{aligned} \quad (26)$$

The calculation of vacuum meson masses from the effective potential also shows that the scale M dependence completely cancels out from their expressions. The explicit derivations of scale independent meson masses are given in the appendix B of Ref. [92].

In general m_π , m_K , the pion and kaon decay constant f_π , f_K , mass squares of η , η' and m_σ are used to fix the six parameters of the model. The parameters are fitted such that in vacuum, the model produces observed pion mass $m_\pi=138$ MeV, kaon mass $m_K=496$ MeV and $m'_\eta = 963$ MeV, $m_\eta = 539$ MeV for constant KMT coupling c . Numerical values of λ_{2s} and c are obtained easily after substituting the values of the input parameters in their expressions in appendix A of Ref. [92]. Numerical values of λ_{2+} and n are obtained using $f_\pi = 92.4$, $f_K = 113$ MeV and $N_c = 3$. The scale independent expressions of m_π^2 and m_σ^2 given in the appendix B of Ref.[92] are exploited in the appendix A of Ref.[92] to obtain the vacuum values of the parameters m^2 and λ_1 using $m_\sigma=400$ MeV. In the present work, the λ_{2s} and c are the same as in the QM model [39], the value of h_x and h_y are also not affected by the fermionic vacuum correction. The parameters which are modified by the fermionic vacuum correction are m^2 , λ_1 and λ_2 . Numerical values of the parameters in the PQMVT model are $c=4807.84$ MeV, $m^2 = (282.67 \text{ MeV})^2$, $\lambda_1 = -8.18$, $\lambda_{2s}=46.48$, $h_x = (120.73 \text{ MeV})^3$ and $h_y = (336.41 \text{ MeV})^3$. We point out that the effect of one loop fermionic vacuum fluctuation in the 2+1 flavor renormalized PQM model, has already been studied in the recent works of Refs. [90, 91]. The model parameters (λ_2 , λ_1 and m^2) in these investigations are renormalization scale dependent and the cancellation of scale dependence for the final results is achieved numerically while we obtain analytical expressions for renormalization scale independent parameters in our model.

Now the thermodynamic grand potential in the presence of appropriately renormalized fermionic vacuum contribution in the Polyakov Quark Meson Model with vacuum term (PQMVT) will be written as

$$\Omega_{\text{MF}}(T, \mu; \sigma_x, \sigma_y, \Phi, \bar{\Phi}) = \mathcal{U}_{\text{Poly-V}}(T; \Phi, \bar{\Phi}) + \Omega(\sigma_x, \sigma_y) + \Omega_{q\bar{q}}^T(T, \mu; \sigma_x, \sigma_y, \Phi, \bar{\Phi}) \quad (27)$$

One can get the quark condensates σ_x , σ_y and Polyakov loop expectation values Φ , $\bar{\Phi}$ by searching the global minima of the grand potential for a given value of temperature T and chemical potential μ .

$$\frac{\partial \Omega}{\partial \sigma_x} = \frac{\partial \Omega}{\partial \sigma_y} = \frac{\partial \Omega}{\partial \Phi} = \frac{\partial \Omega}{\partial \bar{\Phi}} \Big|_{\sigma_x=\bar{\sigma}_x, \sigma_y=\bar{\sigma}_y, \Phi=\bar{\Phi}} = 0. \quad (28)$$

IV. MESON MASSES AND MIXING ANGLES

The curvature of the grand potential in Eq.(14) at the global minimum gives the finite temperature scalar and

pseudo scalar meson masses.

$$m_{\alpha,ab}^2 \Big|_T = \frac{\partial^2 \Omega_{\text{MF}}(T, \mu; \sigma_x, \sigma_y, \Phi, \bar{\Phi})}{\partial \xi_{\alpha,a} \partial \xi_{\alpha,b}} \Big|_{\text{min}} \quad (29)$$

The subscript $\alpha = s, p$; s stands for scalar and p stands for pseudo scalar mesons and $a, b = 0 \dots 8$.

$$m_{\alpha,ab}^2 \Big|_T = m_{\alpha,ab}^2 + (\delta m_{\alpha,ab}^T)^2 \quad (30)$$

The temperature dependence of meson masses comes from the temperature dependence of σ_x and σ_y . The term $(\delta m_{\alpha,ab}^T)^2$ results due to the explicit temperature dependence of quark-antiquark potential in the grand potential. It vanishes in the vacuum where the meson mass matrix is determined as:

$$m_{\alpha,ab}^2 = \frac{\partial^2 \Omega^M(\sigma_x, \sigma_y)}{\partial \xi_{\alpha,a} \partial \xi_{\alpha,b}} \Big|_{\text{min}} = (m_{\alpha,ab}^m)^2 + (\delta m_{\alpha,ab}^v)^2 \quad (31)$$

Here the expressions $(m_{\alpha,ab}^m)^2$ as originally evaluated in Ref. [36, 39], represent the second derivatives of the pure mesonic potential $U(\sigma_x, \sigma_y)$ at its minimum and the vacuum values of meson masses, $m_{\alpha,ab}^2$, in the QM/PQM model are given only by these terms. The calculation details of mass modifications $(\delta m_{\alpha,ab}^v)^2$ resulting due to the fermionic vacuum correction, are presented in the appendix A of Ref.[92] where it has been shown how those expressions are used for determining the model parameters. The Table IV of appendix A in Ref.[92], contains all the expressions of $(m_{\alpha,ab}^m)^2$ and $(\delta m_{\alpha,ab}^v)^2$. The mass expressions $(m_{\alpha,ab}^m)^2$ have a renormalization scale M dependence in the PQMVT model due to the parameter λ_2 . This dependence gets completely canceled by the already existing scale M dependence in the mass modifications $(\delta m_{\alpha,ab}^v)^2$ and the final expressions of vacuum meson masses $m_{\alpha,ab}^2$, are free of any renormalization scale dependence as shown explicitly in the appendix B of Ref.[92].

In order to further calculate the in medium meson mass modifications at finite temperature due to the quark-antiquark contribution in the presence of Polyakov loop potential, the complete dependences of all scalar and pseudo scalar meson fields in Eq.(6) have to be taken into account. We have to diagonalize the resulting quark mass matrix. In the following, we recapitulate the expressions of mass modification due to the quark-antiquark contribution at finite temperature in the PQM model [45] as:

$$\begin{aligned} (\delta m_{\alpha,ab}^T)^2 \Big|_{PQM} &= \frac{\partial^2 \Omega_{q\bar{q}}^T(T, \mu, \sigma_x, \sigma_y, \Phi, \bar{\Phi})}{\partial \xi_{\alpha,a} \partial \xi_{\alpha,b}} \Big|_{\text{min}} \\ &= 3 \sum_{f=x,y} \int \frac{d^3 p}{(2\pi)^3} \frac{1}{E_f} \left[(A_f^+ + A_f^-) \left(m_{f,ab}^2 - \frac{m_{f,a}^2 m_{f,b}^2}{2E_f^2} \right) \right. \\ &\quad \left. + (B_f^+ + B_f^-) \left(\frac{m_{f,a}^2 m_{f,b}^2}{2E_f T} \right) \right] \quad (32) \end{aligned}$$

Here $m_{f,a}^2 \equiv \partial m_f^2 / \partial \xi_{\alpha,a}$ denotes the first partial derivative and $m_{f,ab}^2 \equiv \partial m_{f,a}^2 / \partial \xi_{\alpha,b}$ signifies the second partial derivative of the squared quark mass with respect to the meson fields $\xi_{\alpha,b}$. These derivatives are evaluated in the Table III of Ref. [39]. The notations A_f^\pm and B_f^\pm have the following definitions

$$A_f^+ = \frac{\Phi e^{-E_f^+/T} + 2\bar{\Phi} e^{-2E_f^+/T} + e^{-3E_f^+/T}}{g_f^+} \quad (33)$$

$$A_f^- = \frac{\bar{\Phi} e^{-E_f^-/T} + 2\Phi e^{-2E_f^-/T} + e^{-3E_f^-/T}}{g_f^-} \quad (34)$$

and $B_f^\pm = 3(A_f^\pm)^2 - C_f^\pm$, where we again define

$$C_f^+ = \frac{\Phi e^{-E_f^+/T} + 4\bar{\Phi} e^{-2E_f^+/T} + 3e^{-3E_f^+/T}}{g_f^+} \quad (35)$$

$$C_f^- = \frac{\bar{\Phi} e^{-E_f^-/T} + 4\Phi e^{-2E_f^-/T} + 3e^{-3E_f^-/T}}{g_f^-} \quad (36)$$

In the PQMVT model, the final expression for finite temperature meson masses in Eq. (30) is written as

$$m_{\alpha,ab}^2 \Big|_{T,PQMVT} = m_{\alpha,ab}^2 + (\delta m_{\alpha,ab}^T)^2 \Big|_{PQM} \quad (37)$$

This expression gives meson masses in the PQM model also when the fermionic vacuum contribution becomes zero in the expression of vacuum meson masses in the first term.

The diagonalization of (0,8) component of mass matrix gives the masses of σ and f_0 mesons in scalar sector and the masses of η' and η in pseudo scalar sector. The scalar mixing angle θ_s and pseudo scalar mixing angle θ_p are given by

$$\tan 2\theta_\alpha = \left(\frac{2m_{\alpha,08}^2}{m_{\alpha,00}^2 - m_{\alpha,88}^2} \right) \quad (38)$$

The appendix C of Ref.[39] contains all the transformation details of the mixing for the (0,8) basis that generates the physical basis of the scalar (σ, f_0) and pseudo-scalar (η', η) mesons. This appendix also explains the ideal mixing, and gives the details of formulae by which the physical mesons transform into the mesons which are pure strange or non-strange quark systems.

V. TEMPERATURE DEPENDENCE OF C(T) AND CHIRAL RESTORATION

We are exploring, how the temperature dependence of $U_A(1)$ breaking coupling strength $c(T)$ in the $2 + 1$

flavor Polyakov quark meson model with the fermionic vacuum correction term (PQMVT), influences the chiral symmetry restoration and the axial $U_A(1)$ symmetry restoration. For comparing the results in scenario one, when $U_A(1)$ breaking coupling strength c is constant, we call the PQMVT model as PQMVT-I while in scenario two, when $U_A(1)$ breaking coupling strength $c(T)$ is temperature dependent, we call PQMVT model as PQMVT-II. We have taken two parameter sets for the values of T_1 and b_1 in Eq. (8) for the temperature dependence of $c(T)$. In the first parameter set which we call as model PQMVT-II(a), we have taken $T_1 = .79 T_c$ and $b_1 = .23 T_c$ as obtained in Ref. [93, 94] in the context of fitting a_0 and π meson screening masses to LQCD data [18] in the EPNJL model where they have taken chiral crossover temperature as $T_c = 154$ MeV but we have taken $T_c^x = 169.8$ MeV which is the value of pseudo-critical temperature obtained from the peak of the temperature dependence of non-strange chiral condensate temperature derivative $\frac{\partial \sigma_\pi}{\partial T}$ in the PQMVT model when c is constant. We call this first model set for the temperature dependent $c(T)$ as model PQMVT-II(a) where $T_1 = 134$ MeV and $b_1 = 39$ MeV. In the second parameter set which we call as model PQMVT-II(b), we have taken $T_1 = 111$ MeV = $.66 T_c^x$ and $b_1 = 84.9$ MeV = $.50 T_c^x$ as it fits the Wuppertal group LQCD data for the scaled chiral order parameter which finds $T_c = 157(3)$ [7]. Our model calculation with this parameter set, finds the pseudo-critical temperature for the chiral transition as $T_c = 157.1$ which falls quite well within $T_c = 154 \pm 9$ MeV as reported in Ref. [8].

The interplay of the effect of $U_A(1)$ axial restoration and chiral symmetry restoration due to the temperature dependence of $U_A(1)$ breaking coupling strength $c(T)$, has been investigated in model PQMVT-II(a) and PQMVT-II(b) and compared with the constant c model PQMVT through the temperature variation of strange, non-strange chiral condensates, meson masses and mixing angles. The value of Yukawa coupling $g = 6.5$ has been fixed from the non strange constituent quark mass $m_q = 300$ MeV in vacuum ($T = 0, \mu = 0$). This predicts the vacuum strange quark mass $m_s \simeq 433$ MeV.

A. Effect of $c(T)$ on Condensates

On solving the gap equations Eq.(28) at zero chemical potential, we get the temperature dependence of the Polyakov loop expectation value Φ , non strange and strange condensates. The inflection point of these order parameters respectively give the characteristic temperature (pseudo-critical temperature) for the confinement - deconfinement transition T_c^Φ , the chiral transition in the non-strange T_c^x and strange sector T_s^x . Table I shows the various pseudo-critical temperatures in different models.

For $T = 0$, the condensate $\sigma_{x0} = 92.4$ MeV while

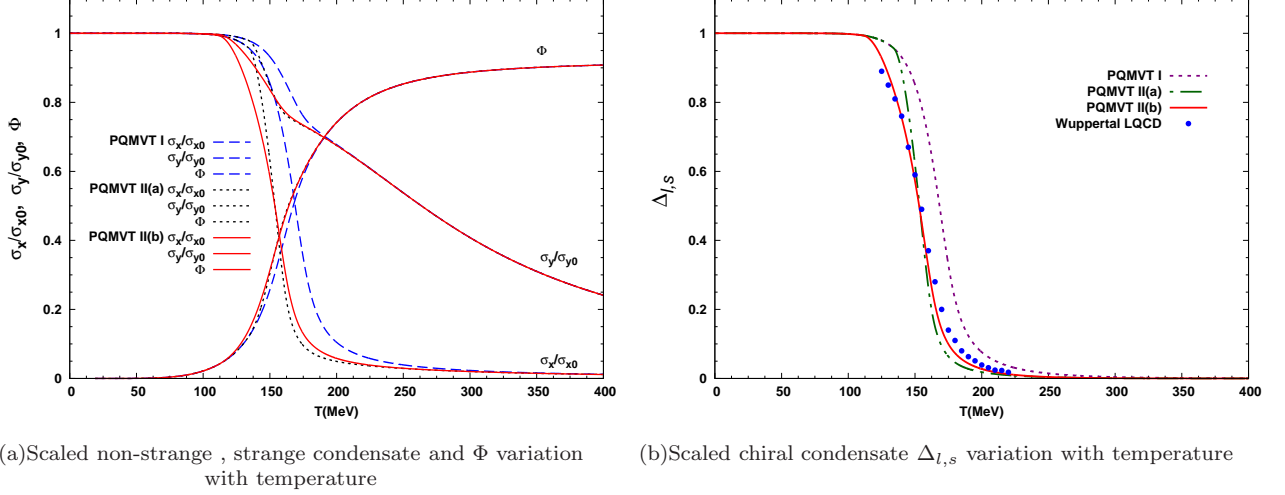


FIG. 1: The Fig.1(a), shows the temperature variations of the scaled non strange condensate ($\frac{\sigma_x}{\sigma_{x0}}$), strange condensate ($\frac{\sigma_y}{\sigma_{y0}}$) on the left side and Polyakov loop field Φ on the right side at zero chemical potential ($\mu = 0$). The dash line in blue, the dotted line in black and the solid line in red respectively, represent the ($\frac{\sigma_x}{\sigma_{x0}}$) temperature variations in the PQMVT-I, PQMVT-II(a) and PQMVT-II(b) model in the lower left part of the Fig. and in the upper left part of the Fig., the same line types respectively, represent the corresponding model ($\frac{\sigma_y}{\sigma_{y0}}$) temperature variations while on the right side of the Fig. the same line types respectively, represent the corresponding model Φ temperature variations. In Fig.1(b), the dotted line in purple, dash double dotted line in green and solid line in red, represent temperature variations of $\Delta_{l,s}$ in PQMVT-I, PQMVT-II(a) and PQMVT-II(b) model respectively. The solid blue dots represent Wuppertal group lattice QCD data.

	PQMVT-I	PQMVT-II(a)	PQMVT-II(b)
T_c^x (MeV)	169.8	155.1	157.1
T_s^x (MeV)	237.3 ± 3.6	239.2 ± 3.5	238.9 ± 3.5
T_c^Φ (MeV)	160.3	151.8	153.1

TABLE I: The table of characteristic temperature (pseudo critical temperature) for the chiral transition in the non-strange sector T_c^x , strange sector T_s^x and the confinement-deconfinement transition T_c^Φ , in the PQMVT-I, PQMVT-II(a) and PQMVT-II(b) models. \pm gives the temperature range near T_s^x over which the rather flat and broad second peak of the strange condensate derivative $\frac{\partial \sigma_y}{\partial T}$, shows a distinct change of about 0.1 percent of the numerical value of the second peak height.

the $\sigma_{y0} = 94.5$ MeV, we have plotted the temperature variations of ($\frac{\sigma_x}{\sigma_{x0}}$), ($\frac{\sigma_y}{\sigma_{y0}}$) and Φ in Fig.1(a). The lower dash line in blue, shows the scaled non-strange condensate temperature variation in the PQMVT-I model for constant c and its inflection point gives the pseudo-critical temperature as $T_c^x = 169.8$ while the upper dash blue line shows the corresponding strange condensate temperature variation. For $c(T)$ with the first parameter set in PQMVT-II(a), the lower dotted line in black shows significant quantitative change in the temperature variation of non-strange condensate when compared to PQMVT-I scenario and its inflection point gives $T_c^x = 155.1$ MeV while the upper black dotted line, shows the corresponding strange condensate temperature variation. In comparison to the

PQMVT-I model, lower solid line in red shows the largest qualitative and quantitative change in the non-strange condensate variation for the second parameter set in PQMVT-II(b) model, corresponding strange condensate variation has also been shown by the upper solid red line and shows the largest change in comparison to the PQMVT-I model for the temperature range 125-200 MeV. For the PQMVT-II(b) model scenario, the inflection point of the non-strange condensate gives pseudo-critical temperature $T_c^x = 157.1$ MeV. The inflection point of the strange condensate in all the three model scenarios, gives almost same pseudo-critical temperature $T_s^x = 237 \rightarrow 239$ MeV because the strange condensate temperature variation shows significant change only in the temperature range 125-200 MeV.

Curves ending in the right side of the Fig.1(a), represent the temperature variation of the Polyakov loop expectation value Φ . Since we have taken $\mu = 0$ in our computations, we get $\Phi = \bar{\Phi}$. We recall that the improved ansatz of the Polyakov loop potential [56] in Eq. (10) avoids the Φ expectation value higher than one. It represents more effective description of the gluon dynamics. The inflection point of the temperature variation of Polyakov loop expectation value, gives confinement-deconfinement transition pseudocritical temperature $T_c^\Phi = 160.3$ MeV, in the PQMVT model while $T_c^\Phi = 151.8$ MeV in the PQMVT-II(a) model and $T_c^\Phi = 153.1$ MeV in the PQMVT-II(b) model scenario. In all the three situations, confinement-deconfinement transition occurs earlier than

the chiral transition as $T_c^\Phi < T_c^\chi$ but this difference is largest of 9.5 MeV for PQMVT-I model with constant c . This difference becomes small of only about 4 MeV in the PQMVT-II(b) model, so the degree of coincidence of the confinement-deconfinement transition with the chiral transition, increases due to the temperature dependence of $c(T)$.

We can not have direct comparison of non-strange condensate $\langle \sigma_x \rangle$ and strange condensate $\langle \sigma_y \rangle$ with the lattice data. First unknown normalization factors are to be removed. $\Delta_{l,s}(T)$ is such observable with the desired chiral limit and it also works as an order parameter for the chiral symmetry breaking. It is written as

$$\Delta_{l,s}(T) = \frac{\langle \sigma_x \rangle(T) - \left(\frac{h_x}{h_y}\right) \langle \sigma_y \rangle(T)}{\langle \sigma_x \rangle(0) - \left(\frac{h_x}{h_y}\right) \langle \sigma_y \rangle(0)} \quad (39)$$

We have shown the temperature variation of the $\Delta_{l,s}(T)$ in the Fig.1(b). We obtained the values of second set of parameters $T_1 = 111 \text{ MeV} = .66 T_c^\chi$ and $b_1 = 84.9 \text{ MeV} = .50 T_c^\chi$ where $T_c^\chi = 169.8 \text{ MeV}$ for the temperature variation of $c(T)$ by fitting the Wuppertal group lattice data for the $\Delta_{l,s}(T)$ [7] to our calculations in model PQMVT-II(b). The solid red line in Fig.1(b) for PQMVT-II(b) model, shows a very good agreement for $\Delta_{l,s}(T)$ temperature variation with lattice QCD data [7]. The first parameter set has been taken from Ref.[93, 94] where they have fitted the a_0 and π meson screening masses to the LQCD data [18] in the context of EPNJL model but results of our calculation with this parameter set in PQMVT-II(a) model, depicted by the double dot dash green line, does not show any agreement with the Wuppertal group lattice data for the $\Delta_{l,s}(T)$. Further the pseudo-critical temperature $T_c^\chi = 157.1 \text{ MeV}$ for the model scenario PQMVT-II(b) matches quite well with the Wuppertal group [7] transition temperature $T_c^\chi = 157(3) \text{ MeV}$ and also falls quite well within the range of pseudo-critical temperature $T_c = 154 \pm 9 \text{ MeV}$ of chiral crossover obtained in Ref. [8]. The purple colour dotted line in Fig.1(b), shows variation of $\Delta_{l,s}(T)$ for constant c scenario in PQMVT-I model.

B. Meson Mass Variations and the $U_A(1)$ Restoration

Temperature variations of the meson masses (σ, π) and (η', a_0) in the PQMVT-I model with constant c has been presented in the left panel (Fig.2(a)) while the corresponding temperature variations for the temperature dependent KMT coupling strength $c(T)$ has been shown in the right panel (Fig.2(b)) for the PQMVT-II(b) model setting. Dash dot line in green shows the temperature variation of π meson, dash line in magenta colour shows the σ mass temperature variation while dash double dotted line in black presents temperature variation of η' meson mass and solid red

line presents temperature variation of a_0 meson mass. Showing the trend of chiral symmetry restoring transition in Fig.2(a) σ degenerates with its chiral partner π near 192 MeV and a_0 meson degenerates with the chiral partner η' near 216 MeV for the PQMVT-I model. Afterwards, the degenerated σ, π meson mass line, shows a converging trend towards the degenerated a_0, η' meson mass line but finally these two lines do not converge for larger temperatures, it means $U_A(1)$ symmetry restoration does not take place in the PQMVT-I model. The Fig.2(b) for the temperature dependent coupling $c(T)$, in the PQMVT-II(b) model shows, in clear contrast to Fig.2(a) that the temperature variations of the masses of the degenerated σ, π meson line completely merges with the temperature variations of the masses of degenerated a_0, η' meson line near 275 MeV. It means that for the parameters of the PQMVT-II(b) model, on account of the mass degeneration of π, a_0, η' and σ , the $U_A(1)$ restoration takes place around 275 MeV which is equal to $1.75 T_c^\chi$. In PQMVT-II(b) model, the mass of σ meson, degenerates with that of π near 181 MeV and mass of a_0 meson, degenerates with that of η' near 185 MeV. We point out that the temperature variation in the mass of η' shows a discontinuous drop of 107 MeV at 174 MeV. This happens because, the temperature variation of the pseudoscalar mixing angle presented later in Fig.4(b) shows a discontinuous jump from -45° to $+45^\circ$ at the same temperature. Corresponding discontinuous jump of 107 MeV in the temperature variation of the mass of η meson is seen exactly at the same temperature in Fig.3(b).

Fig.3(a) in the left panel, shows the temperature variations of masses of (η, f_0) and (K, κ) for the constant c case in the PQMVT model while the right panel Fig.3(b) presents the corresponding temperature variations of masses in the PQMVT-II(b) model for temperature dependent coupling $c(T)$. Dash dot line in green shows the temperature variation of K meson, dash line in magenta colour shows the η mass temperature variation while dash double dotted line in black presents temperature variation of κ meson mass and solid red line presents temperature variation of f_0 meson mass. Mass variation lines of K, κ and η almost merge with each other near 339 MeV while f_0 meson mass variation almost merges with these degenerated three lines near 383 MeV in the PQMVT-I model. In contrast, in Fig.3(b) in the right panel, for the temperature dependent KMT coupling $c(T)$ in the PQMVT-II(b) model, mass variation lines of K, κ and η merge early with each other near 255 MeV while f_0 meson mass variation merges with these degenerated three lines near 351 MeV. f_0 meson mass variation is similar in PQMVT-I and PQMVT-II(b) models. This happens because most of the changes due to temperature dependent parameterizations of KMT coupling strength $c(T)$ takes place in the temperature range 125 MeV to 200 MeV. The melting trend of the strange condensate variation after 200 MeV in Fig.1(a)

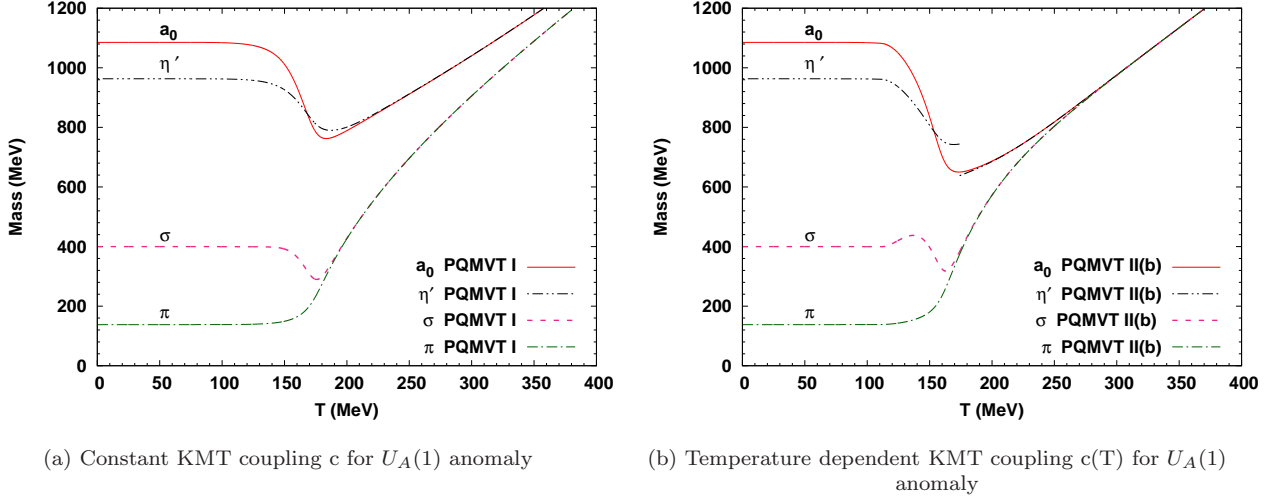


FIG. 2: Shows the mass variations for the (π, σ) and (η', a_0) with respect to the temperature at zero chemical potential ($\mu = 0$). Fig.2(a) shows the results for the PQMVT-I model and the line types for mass variations are labeled. Fig.2(b) shows the mass variations for the PQMVT-II(b) model with labeled line types.

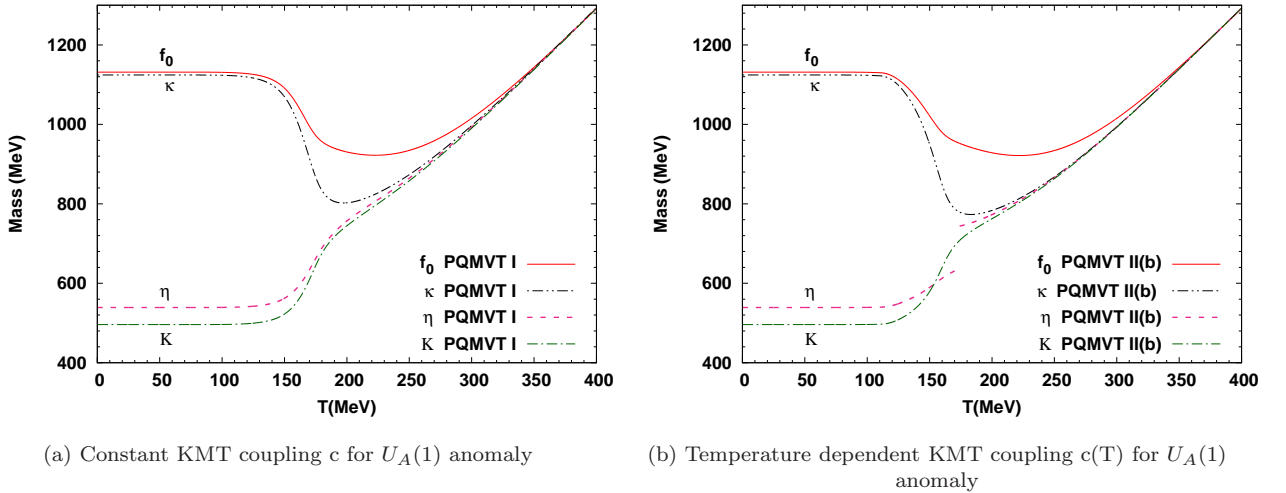


FIG. 3: Shows the mass variations for the (K, κ) and (η, f_0) with respect to the temperature at zero chemical potential ($\mu = 0$). Fig.3(a) shows the results for the PQMVT-I model and the line types for mass variations are labeled. Fig.3(b) shows the mass variations for the PQMVT-II(b) model with labeled line types.

in PQMVT-I with constant c matches almost exactly with the corresponding strange condensate variation trend in PQMVT-II(a) and PQMVT-II(b) models for temperature dependent coupling $c(T)$. In Fig.3(b), we see that the mass variation of the η meson shows jump at 174 MeV, exactly the same temperature at which mass variation of η' meson shows a drop in Fig.3(b).

C. Meson Mixing Angle Variations

We will now be exploring the nature of the scalar θ_s and pseudo scalar θ_p mixing angles temperature variations.

In Fig.4(a) in the left panel, the dash dotted line in green shows the pseudoscalar mixing angle θ_p temperature variations while the solid line in red shows scalar mixing angle θ_s temperature variations for the PQMVT-I model with constant coupling c . In Fig.4(b) in the right panel, the same line types respectively show the θ_p and θ_s temperature variations for the PQMVT-II(b) model with temperature dependent KMT coupling $c(T)$. As in Refs. [39, 45, 92], in the low temperature chiral symmetry broken phase, the nonstrange and strange quark mixing is strong and one gets almost constant pseudoscalar mixing angle $\theta_p = -5^\circ$ in both the Fig.4(a) and Fig.4(b). As temperature increases near 150 MeV, the θ_p variation in the PQMVT-I

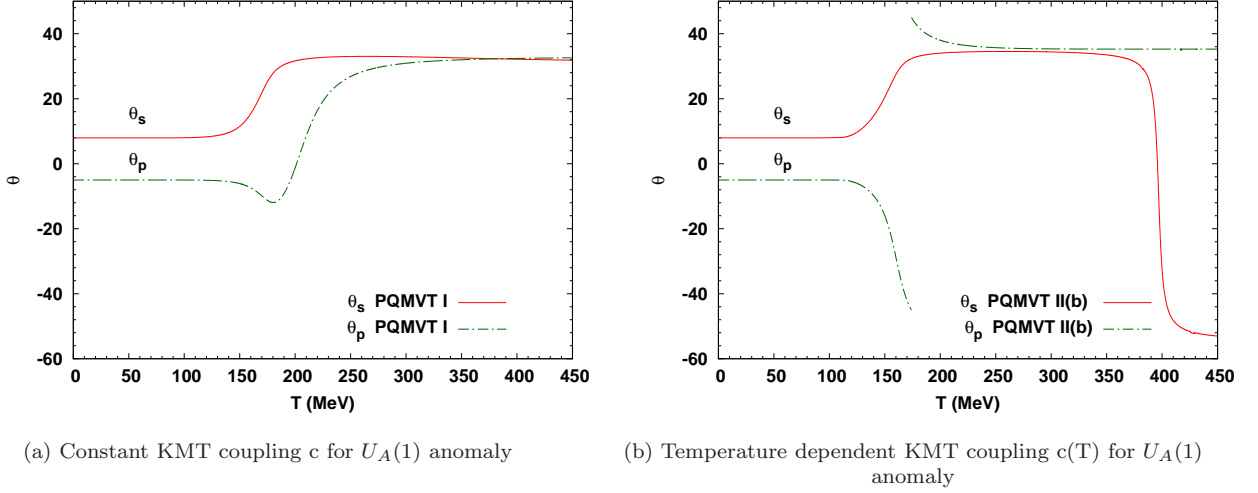


FIG. 4: Shows the temperature variations of pseudoscalar mixing angle θ_p and scalar mixing angle θ_s at zero ($\mu = 0$) chemical potential. Fig.4(a) shows the results for the PQMVT-I model and the line types for mixing angle variations are labeled. Fig.4(b) shows the mixing angle variations for the PQMVT-II(b) model with labeled line types.

model develops a dip around pseudocritical temperature $T_c^x = 169.8$ MeV and then smoothly starts approaching the ideal mixing angle $\theta_p \rightarrow \arctan \frac{1}{\sqrt{2}} \sim 35^\circ$ in the high temperature chiral symmetry restored phase. In PQMVT-II(b) model, in complete contrast, in Fig.4(b), the θ_p variation starts a sharp dip after 120 MeV due to the effect of the temperature dependent coupling $c(T)$ and at 174 MeV, the pseudoscalar mixing angle θ_p discontinuously jumps from -45° to $+45^\circ$ and then starts approaching ideal mixing angle 35° in the high temperature chiral symmetry restored phase. The effect of this discontinuous jump in θ_p is seen in the discontinuous fall in the mass of η' meson in Fig.2(b) and the corresponding jump in the mass of η meson exactly by the same amount of 107 MeV in Fig.3(b). It means after this discontinuous jump in θ_p , η' and η mesons change their identity.

The scalar mixing angle θ_s in vacuum ($T = 0$) is 8° in both the cases of PQMVT-I model and PQMVT-II(b) model situations in Fig.4(a) and Fig.4(b) respectively. The θ_s starts growing towards its ideal value for temperature about 10 MeV higher than the $T_c^x = 169.8$ MeV, in the PQMVT-I model in Fig.4(a) and approaches the ideal mixing angle very smoothly in the higher temperature chirally symmetric phase. The effect of temperature dependent coupling $c(T)$ modifies the temperature variation of scalar mixing angle θ_s in the PQMVT-II(b) model. Here, the θ_s starts approaching its ideal value for temperature about 10 MeV higher than the $T_c^x = 157.1$ MeV in Fig.4(b) and for higher temperatures in the chirally symmetric phase, the scalar mixing angle first achieves its ideal value 35° and then drops down to $\theta_s \sim -53^\circ$ for about 450 MeV temperature. This pattern is already reported and discussed in Ref.[39, 45] for the Quark Meson (QM)

model and Polyakov Quark Meson (PQM) model.

Ideal pseudo scalar mixing gets fully achieved for temperatures above 180 MeV in chiral symmetric phases of both the models i.e PQMVT-I model in Fig.4(a) and PQMVT-II(b) model in Fig.4(b). In consequence, the η and η' mesons become a purely strange η_S and non strange η_{NS} quark system. In order to show this and make comparisons, we have plotted the temperature variations of the masses of physical η , η' and the non strange-strange η_{NS} , η_S mass complex, for the PQMVT-I model in Fig.5(a) and PQMVT-II(b) model plots are given in Fig.5(b). Mass formula for $m_{\eta_{NS}}$ and m_{η_S} are given in the Table V of appendix B of Ref.[92]. The $m_{\eta'}$ variation shown by the red line merges with $m_{\eta_{NS}}$ variation depicted by the dash double dot green line near 221 MeV in PQMVT-I model in Fig.5(a) while the m_η variation shown by the dash dot black line merges with the m_{η_S} variation shown by the dash line in magenta near the same temperature but these two degenerated lines do not meet with each other. The $m_{\eta'}$ variation in the PQMVT-II(b) model shows a discontinuous drop of about 107 MeV in its mass in Fig.5(b) at 174 MeV temperature and then it becomes degenerate with $m_{\eta_{NS}}$ temperature variation while the m_η temperature variation shows discontinuous jump by the same amount of 107 MeV in its mass at 174 MeV and afterwards it becomes degenerate with m_{η_S} temperature variation. In PQMVT-II(b) model, the discontinuous drop in $m_{\eta'}$ variation and the discontinuous jump in m_η variation by the same amount exactly at the same temperature of 174 MeV, takes place because the pseudoscalar mixing angle θ_p in Fig.4(b) registers a discontinuous jump from -45° to $+45^\circ$. In complete contrast to Fig.5(a) of PQMVT-I model, the $m_{\eta'}$ and $m_{\eta_{NS}}$ degenerated lines further become degenerate with the m_η and m_{η_S} degenerated lines i.e. all the four lines merge with each other near

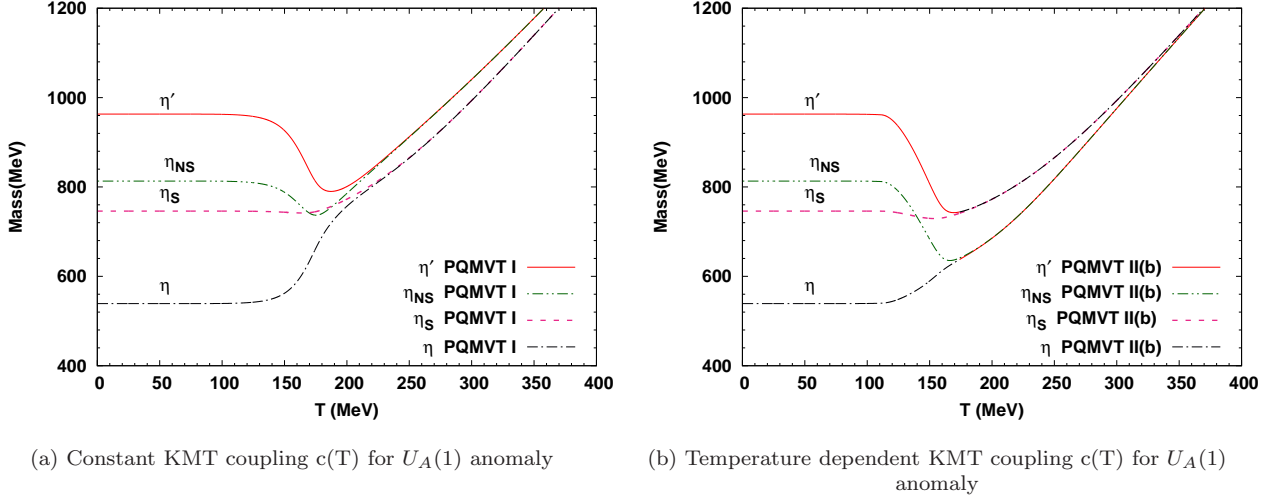


FIG. 5: Shows the mass variations for the physical η' , η and the non strange-strange η_{NS} , η_S complex, with respect to temperature at zero chemical potential ($\mu = 0$). Fig.5(a) shows the results for PQMVT-I model and line types for mass variations are labeled. Fig.5(b) shows the mass variations for the PQMVT-II(b) model with labeled line types.

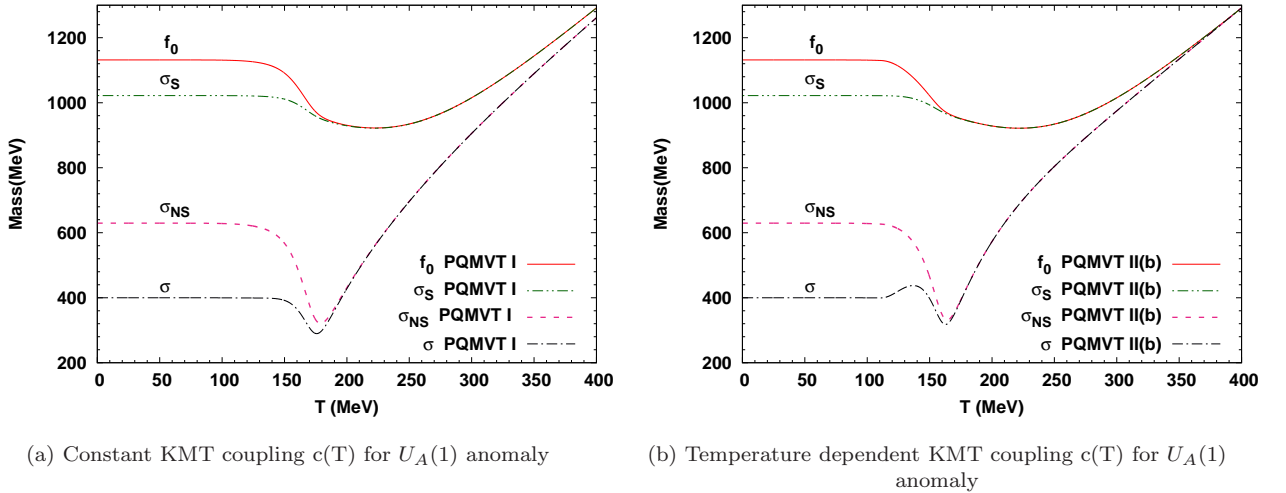


FIG. 6: Shows the mass variations for the (σ, σ_{NS}) and for the (f_0, σ_S) , with respect to temperature at zero chemical potential ($\mu = 0$). Fig.6(a) shows the results for PQMVT-I model and line types for mass variations are labeled. Fig.6(b) shows the mass variations for the PQMVT-II(b) model with labeled line types.

360 MeV in Fig.5(b) for the PQMVT-II(b) model. It means complete $U_A(1)$ restoration takes place in the PQMVT-II(b) model near 360 MeV.

In Fig.6(a) for the PQMVT-I model, we notice that the f_0 meson mass temperature variation shown by the solid red line degenerates with the pure strange quark system σ_S mass temperature variation shown by the green double dot dash line near 186 MeV while the σ meson mass temperature variation shown by the black dash dot line becomes identical with the pure non-strange quark system σ_{NS} mass variation shown by the magenta dash line near the temperature 197 MeV. Further these two degenerated lines show mass convergence trend but do not merge with each

other, it means $U_A(1)$ restoration does not take place in the PQMVT-I model. For temperature dependent coupling $c(T)$ in the PQMVT-II(b) model, in Fig.6(b), we find that the f_0 meson mass temperature variation degenerates with the pure strange quark system σ_S mass temperature variation near 165 MeV and the σ meson mass temperature variation merges with the pure non-strange quark system σ_{NS} mass variation near the temperature 171 MeV. In quite contrast to PQMVT-I model, these two degenerated lines show a strong mass convergence trend and further merge with each other near 370 MeV temperature, it means complete $U_A(1)$ restoration takes place in the PQMVT-II(b) model.

VI. SUMMARY AND CONCLUSION

In the present work, we have explored, how the temperature dependence of KMT coupling strength $c(T)$ in the PQMVT model, modifies the interplay of chiral symmetry and the $U_A(1)$ symmetry restoration. For comparing the results, when coupling strength c is constant, we call the PQMVT model as PQMVT-I while for temperature dependent coupling $c(T)$, we call the PQMVT model as PQMVT-II. We have taken two parameter sets for the temperature dependence of $c(T)$ but for comparison, we focus on the PQMVT-II(b) model for the second parameter set as it fits the LQCD data for the scaled chiral order parameter $\Delta_{l,s}(T)$ from which Wuppertal group obtained the pseudo-critical temperature for chiral transition as $T_c = 157(3)$ MeV [7]. In comparison to the PQMVT-I model for constant c , the largest qualitative and quantitative change in the non-strange condensate temperature variation, is seen in the model PQMVT-II(b), corresponding strange condensate variation has also been found to be the largest for the temperature range 125-200 MeV. The chiral crossover temperature for the nonstrange sector is $T_c^x = 169.8$ MeV in PQMVT-I model while $T_c^x = 157.1$ MeV for the model PQMVT-II(b) scenario which matches with Wuppertal lattice result $T_c = 157(3)$ MeV and also falls quite well within $T_c = 154 \pm 9$ MeV as reported in Ref. [8]. Confinement-deconfinement transition occurs earlier than the chiral transition as $T_c^\Phi < T_c^x$ in all the calculations but this difference is largest of 9.5 MeV for PQMVT-I model with constant c . This difference becomes small of only about 4 MeV in the PQMVT-II(b) model, so the degree of coincidence of the confinement-deconfinement transition with the chiral transition, increases due to the temperature dependence of $c(T)$.

Showing chiral symmetry restoration σ , π mass degenerates near the temperature of 192 MeV while a_0 mass degenerates with the η' meson mass near 216 MeV in PQMVT-I model but the degenerated σ , π meson mass line, do not converge for larger temperatures with the degenerated a_0 , η' meson mass line, it means $U_A(1)$ symmetry restoration does not take place in the PQMVT-I model. For the temperature dependent coupling $c(T)$, in the PQMVT-II(b) model, σ , π mass degenerates near 181 MeV while a_0 mass degeneration with the η' mass happens near 186 MeV and the degenerated σ , π meson mass line merges with the temperature variations of the masses of degenerated a_0 , η' mesons near 275 MeV. It means, the $U_A(1)$ restoration takes place around 275 MeV = $1.75 T_c^x$ in the PQMVT-II(b) model in complete contrast to PQMVT-I model. Mass variation lines of K , κ and η become almost degenerate with each other near 339 MeV while f_0 meson mass variation almost merges with these degenerated three lines near 383 MeV in PQMVT-I model. In contrast, for the temperature dependent KMT coupling $c(T)$ in the PQMVT-II(b) model, mass variation lines of

K , κ and η merge early with each other near 255 MeV while f_0 meson mass variation almost merges with these degenerated three lines near 351 MeV.

The pseudoscalar mixing angle θ_p temperature variation in the PQMVT-I model develops a dip near pseudocritical temperature $T_c^x = 169.8$ MeV and then smoothly approaches the ideal mixing angle $\theta_p \rightarrow \arctan \frac{1}{\sqrt{2}} \sim 35^\circ$ in the high temperature chiral symmetry restored phase. In PQMVT-II(b) model, in complete contrast, the θ_p variation starts a sharp dip after 120 MeV due to the effect of the temperature dependent coupling $c(T)$ and at 174 MeV, the pseudoscalar mixing angle θ_p discontinuously jumps from -45° to $+45^\circ$ and then starts approaching ideal mixing angle 35° in the high temperature chiral symmetry restored phase. The effect of this discontinuous jump in θ_p in PQMVT-II(b) model, gets reflected in the discontinuous drop of 107 MeV in the mass of η' meson and the corresponding jump in the mass of η meson exactly by the same amount at 174 MeV temperature. The scalar mixing angle θ_s starts growing towards its ideal value for temperature about 10 MeV higher than the $T_c^x = 169.8$ MeV, in the PQMVT-I model and approaches the ideal mixing angle very smoothly in the higher temperature chirally symmetric phase. The effect of temperature dependent coupling $c(T)$ modifies the temperature variation of scalar mixing angle θ_s in the PQMVT-II(b) model. Here, the θ_s starts approaching its ideal value for temperature about 10 MeV higher than the $T_c^x = 157.1$ MeV, and for higher temperatures in the chirally symmetric phase, the scalar mixing angle first achieves its ideal value 35° and then drops down to $\theta_s \sim -53^\circ$ for about 450 MeV temperature.

In complete contrast to PQMVT-I model, the $m_{\eta'}$ and $m_{\eta_{NS}}$ degenerated lines further become degenerate with the m_η and m_{η_S} degenerated lines i.e. all the four lines merge with each other near 361 MeV for the PQMVT-II(b) model. It means complete $U_A(1)$ restoration takes place in the PQMVT-II(b) model due to the temperature dependence of KMT coupling $c(T)$ while this does not happen in the PQMVT-I model. Confirming this trend, we find that the f_0 meson mass and the pure strange quark system σ_S mass degenerated lines further merge with the degenerated σ meson mass and the pure non-strange quark system σ_{NS} mass temperature variation lines near 370 MeV while this kind of thing does not happen in the PQMVT-I model.

Acknowledgments

Computational support of the computing facility which has been developed by the Nuclear Particle Physics group of the Physics Department, Allahabad University under the Center of Advanced Studies (CAS) funding of UGC, India, is acknowledged.

-
- [1] E.V.Shuryak Phys. Rep. **61**, 71 (1980); *ibid* **115**, 151 (1984).
- [2] J. Rafelski Phys. Rep. **88**, 331 (1982); *ibid* **142**, 167-262 (1986).
- [3] L.D.McLerran, B.Svetitsky, Phys. Rev. D **24**, 450 (1981); B.Svetitsky, Phys. Rep. **132**, 1 (1986).
- [4] B.Muller, Rep. Prog. Phys. **58**, 611 (1995).
- [5] H.Meyer-Ortmanns Rev. Mod. Phys. **68**, 473 (1996).
- [6] D. H. Rischke, Prog. Part. Nucl. Phys. **52**, 197 (2004).
- [7] S. Borsanyi, Z. Fodor, C. Hoelbling, S. D. Katz, S. Krieg, C. Ratti and K. K. Szabo, JHEP **1009**, (2010) 073 ; arXiv:1005.3508 [hep-lat].
- [8] A. Bazavov, T. Bhattacharya, M. Cheng, C. DeTar, H. T. Ding, S. Gottlieb, R. Gupta and P. Hegde *et al.*, Phys. Rev. D **85**, 054503 (2012); arXiv:1111.1710 [hep-lat].
- [9] K. Kanaya, AIP Conf. Proc. **1343**, 57 (2011); Proc. Sci., LATTICE2010 (2010) 012 .
- [10] G. 't Hooft, Phys. Rev. Lett. **37**, 8 (1976);
- [11] M.Kobayashi and T.Maskawa, Prog. Theor. Phys. **44**, 1422 (1970); M.Kobayashi, H. Kondo and T.Maskawa, Prog. Theor. Phys. **45**, 1955 (1971). Phys. Rev D **14**, 3432 (1976); Phys. Rev D **18**, 2199(E) (1978) .
- [12] D. J. Gross, R. D. Pisarski, and L. G. Yaffe, Rev. Mod. Phys. **53**, 43 (1981) .
- [13] T. Schafer and E. V. Shuryak , Rev. Mod. Phys. **70**, 323 (1998) .
- [14] E. V. Shuryak, Comments Nucl. Part. Phys. **21**, 235 (1994).
- [15] J. I. Kapusta, D. Kharzeev, and L. D. McLerran, Phys. Rev. D **53**, 5028 (1996).
- [16] T. Csorgo, R. Vertesi, and J. Sziklai, Phys. Rev. Lett. **105**, 182301 (2010).
- [17] R. Vertesi, T. Csorgo, and J. Sziklai, Phys. Rev. C **83**, 054903 (2011).
- [18] M. Cheng, S. Datta, A. Francis, J. van der Heide, C. Jung, O. Kaczmarek, F. Karsch, E. Laermann, R. D. Mawhinney, C. Miao *et al.*, Eur. Phys. J. C **71**, 1564 (2011).
- [19] G. Cossu, S. Aoki, H. Fukaya, S. Hashimoto, T. Kaneko, H. Matsuferu and J.-i. Noaki, Phys. Rev. D **87** 114514 (2013); **88** 019901(E) (2013).
- [20] G. Cossu, H. Fukaya, S. Hashimoto, J.-i. Noaki and A. Tomiya (JLQCD collaboration), *Proc. Sci.*, LATTICE2015(2016) 196 [arXiv:1511.05691].
- [21] T. Bhattacharya *et al.*, Phys. Rev. Lett. **113**, 082001 (2014).
- [22] A. Bazavov, *et al.* (HotQCD Collaboration Phys. Rev. D **86**, 094503 (2012).
- [23] S. Sharma, V. Dick, F. Karsch, E. Laermann, and S. Mukherjee, *Proc. Sci.*, LATTICE2013 (2014) 164 [arXiv:1311.3943].
- [24] V. Dick, F. Karsch, E. Laermann, and S. Mukherjee, and S. Sharma, Phys. Rev. D **91**, 094504 (2015).
- [25] L. von Smekal, A. Mecke, and R. Alföker, AIP Conf. Proc. **412**, 746 (1997).
- [26] R. Alföker, C. S. Fischer, and R. Williams, Eur. Phys. J. A **38**, 53 (2008).
- [27] S. Benic, D. Horvatic, D. Kekez, and D. Klabucar, Phys. Rev. D **84**, 016006 (2011).
- [28] S. Benic, D. Horvatic, D. Kekez, and D. Klabucar, Phys. Lett. B **738**, 113 (2014).
- [29] P. Costa, M. C. Ruivo, C. A. de Sousa and Yu. L. Kalinovsky Phys. Rev. D **70**, 116013 (2004).
- [30] P. Costa, M. C. Ruivo, C. A. de Sousa and Yu. L. Kalinovsky Phys. Rev. D **71**, 116002 (2005).
- [31] J.-W. Chen, K. Fukushima, H. Kohyama, K. Ohnishi, and U. Raha ,Phys. Rev. D **80**, 054012 (2009).
- [32] Z. Zhang and T. Kunihiro , Phys. Rev. D **83**, 114003 (2011).
- [33] P. D. Powell and G. Byam, Phys. Rev. D **85**, 074003 (2012).
- [34] N. M. Bratovic, T. Hatsuda, and W. Weise Phys. Lett. B **719**, 131 (2013).
- [35] J. Schaffner-Bielich, Phys. Rev. Lett. **84**, 3261 (2000).
- [36] J. T. Lenaghan, D. H. Rischke and J. Schaffner-Bielich, Phys. Rev D **62**, 085008 (2000).
- [37] G. Fejos, Phys. Rev. D **92**, 036011 (2015) .
- [38] J. Eser, M. Grahel and D. H. Rischke, Phys. Rev. D **92**, 096008 (2015).
- [39] B. J. Schaefer and M. Wagner, Phys. Rev. D **79**, 014018 (2009).
- [40] B. J. Schaefer and M. Wagner, Prog.Part.Nucl.Phys. **62**, 381 (2009)
- [41] M. Mitter and B. J. Schaefer, Phys. Rev. D **89**, 054027 (2014).
- [42] T. K. Herbst, M. Mitter, J. M. Pawlowski, B.-J. Schaefer, and R. Stiele Phys. Lett. B **731**, 248 (2014).
- [43] B. J. Schaefer, J. M. Pawlowski and J. Wambach, Phys. Rev. D **76**, 074023 (2007)
- [44] J. Braun and H. Gies Phys. Lett. B **645** 53 (2007); JHEP **06**, 024 (2006)
- [45] U. S. Gupta and V. K.Tiwari, Phys. Rev. D **81**, 054019 (2010).
- [46] B. J. Schaefer, M. Wagner and J. Wambach, Phys. Rev. D **81**, 074013 (2010)
- [47] B. J. Schaefer, M. Wagner and J. Wambach, Proc. Sci., **CPOD2009**, 017 (2009).
- [48] H. Mao, J. Jin and M. Huang, J. Phys. G **37**, 035001 (2010).
- [49] T. K. Herbst, J. M. Pawlowski, and B.-J. Schaefer. Phys. Lett. B **696**, 58 (2011).
- [50] B.-J. Schaefer, arXiv:1102.2772 [hep-ph]; J. M. Pawlowski, AIP Conf. Proc. **1343**, 75 (2011)
- [51] G. Marko and Zs. Szep, Phys. Rev. D **82**, 065021 (2010).
- [52] T. Kahara and K. Tuominen, Phys. Rev. D **78**, 034015 (2008); *ibid* D **80**, 114022 (2009). *ibid* D **82**, 114026 (2010).
- [53] S. Digal, E. Laermann and H. Satz, Eur. Phys. J. C **18**, 583 (2001).
- [54] Claudia Ratti, Michael A. Thaler and Wolfram Weise, Phys. Rev. D **73**, 014019 (2006).
- [55] S. Rößner, C. Ratti, and W. Weise, Phys. Rev. D **75**, 034007 (2007).
- [56] S. K. Ghosh, T. K. Mukherjee, M. G. Mustafa and R. Ray Phys. Rev. D **77**, 094024 (2008).
- [57] H. Hansen, W. M. Alberico, A. Beraudo, A. Molinari, M. Nardi and C. Ratti, Phys. Rev. D **75**, 065004 (2007).
- [58] S. Rößner, T. Hell, C. Ratti, and W. Weise, Nucl. Phys. A **814**, 118 (2008).
- [59] S. K. Ghosh, T. K. Mukherjee, M. G. Mustafa and R. Ray, Phys. Rev. D **73**, 114007 (2006).

- [60] P. Costa, M. C. Ruivo, C. A. de Sousa, H. Hansen and W. M. Alberico Phys. Rev. **D 79**, 116003 (2009).
- [61] C. Sasaki, B. Friman and K. Redlich, Phys. Rev **D 75**, 074013 (2007).
- [62] T. Hell, S. Rößner, M. Cristoforetti and W. Weise, Phys. Rev **D 79**, 014022 (2009).
- [63] H. Abuki, R. Anglani, R. Gatto, G. Nardulli and M. Ruggieri, Phys. Rev **D 78**, 034034 (2008).
- [64] M. Ciminale, R. Gatto, N. D. Ippolito, G. Nardulli and M. Ruggieri, Phys. Rev **D 77**, 054023 (2008).
- [65] W.-J. Fu, Z. Zhang and Y.-X. Liu, Phys. Rev **D 77**, 014006 (2008).
- [66] K. Fukushima, Phys. Lett. **B 591**, 277 (2004).
- [67] K. Fukushima, Phys. Rev **D 77**, 114028 (2008).
- [68] K. Fukushima, Phys. Rev **D 78**, 114019 (2008).
- [69] K. Fukushima, Phys. Rev **D 79**, 074015 (2009).
- [70] G. A. Contrera, M. Orsaria, and N. N. Scoccola, Phys. Rev. **D 82**, 054026 (2010).
- [71] A. E. Radzhabov, D. Blaschke, M. Buballa, and M. K. Volkov, Phys. Rev. **D 83**, 116004 (2011)
- [72] O. Lourenco, M. Dutra, T. Frederico, A. Delfino, M. Malheiro Phys.Rev. **D 85**, 097504 (2012); O. Lourenco, M. Dutra, A. Delfino, M. Malheiro Phys.Rev. **D 84**, 125034 (2011).
- [73] G. A. Contrera, D. Gomez Dumm and Norberto N. Scoccola, Phys. Rev. **D 81**, 054005 (2010).
- [74] A. A. Asipov, B. Hiller and Joao Da Providencia, Phys.Lett. **B 634**, 48-54 (2006); A. A. Asipov, B. Hiller, A. H. Blin and Joao Da Providencia, Annals Phys. (Amsterdam) **322**, 2021 (2007); A. A. Asipov, B. Hiller, J. Moreira, A. H. Blin and Joao Da Providencia, Phys.Lett. **B 646**, 91-94 (2007); A. A. Asipov, B. Hiller, J. Moreira and A. H. Blin, Phys.Lett. **B 659**, 270-274 (2008); B. Hiller, J. Moreira, A. A. Asipov and A. H. Blin, Acta Phys.Polon.Supp. **5**, 1171-1177 (2012).
- [75] A. M. Polyakov, Phys. Lett. **B 72**, 477 (1978).
- [76] R. D. Pisarski, Phys. Rev. **D 62** 111501(R) (2000).
- [77] B. Layek, A. P. Mishra, A. M. Srivastava and V. K. Tiwari, Phys. Rev. **D 73** 103514 (2006).
- [78] E. Meggiolaro and A. Morda Phys. Rev. **D 88** 096010 (2013).
- [79] K. Fukushima, K. Ohnishi, K. Ohta, Phys. Rev **C 63**, 045203 (2001).
- [80] V. Skokov, B. Friman, E. Nakano, K. Redlich, and B.-J. Schaefer, Phys. Rev. **D 82**, 034029 (2010)
- [81] R. D. Pisarski and F. Wilczek Phys. Rev. **D 29**, 338 (1984).
- [82] A. J. Mizher, M. N. Chernodub and E. S. Fraga, Phys. Rev. **D 82**, 105016 (2010).
- [83] L. F. Palhares and E. S. Fraga, Phys. Rev. **D 78**, 025013 (2008) [arXiv:0803.0262 [hep-ph]].
- [84] E. S. Fraga, L. F. Palhares and M. B. Pinto, Phys. Rev. **D 79**, 065026 (2009) [arXiv:0902.1498 [hep-ph]].
- [85] L. F. Palhares and E. S. Fraga, Phys. Rev. **D 82**, 125018 (2010) [arXiv:1006.2357 [hep-ph]].
- [86] Yin Jiang, Tao Xia and Pengfei Zhuang Phys. Rev. **D 93**, 074006 (2016).
- [87] Markus Heller and Mario Mitter Phys. Rev. **D 94**, 074002 (2016).
- [88] U. S. Gupta and V. K. Tiwari, Phys. Rev. **D 85**, 014010 (2012).
- [89] Vivek Kumar Tiwari, Phys. Rev. **D 86**, 094032 (2012).
- [90] B.-J. Schaefer and M. Wagner, Phys. Rev. **D 85**, 034027 (2012).
- [91] Sandeep Chatterjee, Kirtimaan A. Mohan Phys.Rev. **D 85**, 074018 (2012); *ibid* **D 86**, 114021 (2012).
- [92] V. K. Tiwari Phys. Rev. **D 88** 074017 (2013).
- [93] M. Ishii, K. Yonemura, J. Takahashi, H. Kouno and M. Yahiro Phys. Rev. **D 93** 016002 (2016).
- [94] M. Ishii, H. Kouno and M. Yahiro Phys. Rev. **D 95** 114022 (2017).
- [95] R. D. Pisarski and L. G. Yaffe Phys. Lett. **97B**, 110 (1980).
- [96] Finite Temperature Field Theory Principles and Applications, J. I. Kapusta and C. Gale, Cambridge University Press.
- [97] M. Quiros, in Proceeding: The Summer School in High Energy Physics and Cosmology, ICTP Series in Theoretical Physics, Trieste, Italy, 1998, edited by A. Masiero, G. Senjanovic, and A. Smirnov (World Scientific, Singapore, 1999), Vol. 15, p. 436.